Sentinel-3 SAR Mode altimetry observations of wave breaking dissipation owing to large-amplitude Internal Solitary Waves: effects on SWH and radar backscatter

Adriana M. Santos Ferreira[1,2] , José C. B. da Silva[2,3] , Jorge M. Magalhaes[1,2] , Thomas Moreau[4] , Claire Maraldi[5] , Franck Borde[6] , Craig Donlon[6]

(1) CIIMAR – Interdisciplinary Centre of Marine and Environmental Research, Avenida Gerenal Norton de Matos s/n, 4450-208, Porto, Portugal
(2) Department of Geosciences, Environment and Spatial Planning (DGAOT), Faculty of Sciences, University of Porto, rua do Campo Alegre s/n, 4169-007 Porto, Portugal
(3) ICT – Institute of Earth Sciences, Rua Romão Ramalho, 59, 7002-554 Évora, Portugal
(4) CLS - Collect Localisation Satellites, 11 Rue Hermès, Parc Tecnologique du Canal, 31520 Ramonville St Agne, France
(5) CNES – Centre National d'Études Spatiales, 18 avenue Edouard Belin, 31401 Toulouse Cedex 9, France
(6) ESA/ESTEC - European Space Research and Technology Centre, Keplerlaan, 1, 2201 AZ Noordwijk, The Netherlands

We address surface wave breaking caused by oceanic Internal Solitary Waves (ISWs) and how ISWs are manifested in the SAR altimeter onboard Sentinel-3A and 3B satellites, by means of their effects in Significant Wave Height (SWH). Furthermore, it has been recently shown that ISWs are successfully detected by using satellite altimetry (Santos-Ferreira et al., 2018; 2019). Here, we select two different regions of the ocean, namely the tropical Atlantic Ocean off the Amazon shelf and the Banda Sea in the Indian Ocean, where there are scenes of Sentinel-3 OLCI (Ocean Land Colour Instrument) acquired simultaneously with along-track SAR mode altimeter, which included signatures of large amplitude ISWs.

New data of unfocused SAR (UF SAR 20 Hz) and fully focused SAR (FF SAR 160 Hz) modes is analysed, which are retracked in full range and over a reduced range of bins (truncation carried out dynamically ten gates away from the estimated epoch position). Such an adaptive retracking algorithm that additionally estimates a constant mean square slope has been developed and applied in this study, abbreviated as MSS (see some results of these new advanced products in Fig. 2). It has been observed a strong decrease in normalized radar cross section (NRCS) over the rough part of the ISWs, and a small increase in the smooth part relatively to the unperturbed ocean background (Santos-Ferreira et al., 2018). Moreover, we demonstrate that the Significant Wave Height (SWH) parameter is significantly attenuated, after the passage of an ISW, considering length scales of about 10 km before and after the ISW crest, i.e. in 20 km length scales (see Figs. 1 and 2). It is suggested that the cause of this SWH attenuation is related to the wave breaking associated with the ISWs, characterized by surface wave energy dissipation, turbulence effects and air emulsion.

Furthermore, Sentinel-2 images are analysed and provide insights admittedly into this same phenomenon: white-capping of two different kinds are reported, the first being a traditional radiance increase at all (visible) wavelengths extended in time scales of tens of seconds, and a second kind associated to quick transient "flashes" of enhanced radiance depicted in different coloured pixels in RGB composite images, with typical time scales of one second or less (Figs. 3 and 4). We follow the methods published in Kubryakov et al., 2021. Fraction of modulation of breaking waves in the presence of internal waves are presented (Fig. 5).

Surface wave breaking induced by strong ISWs

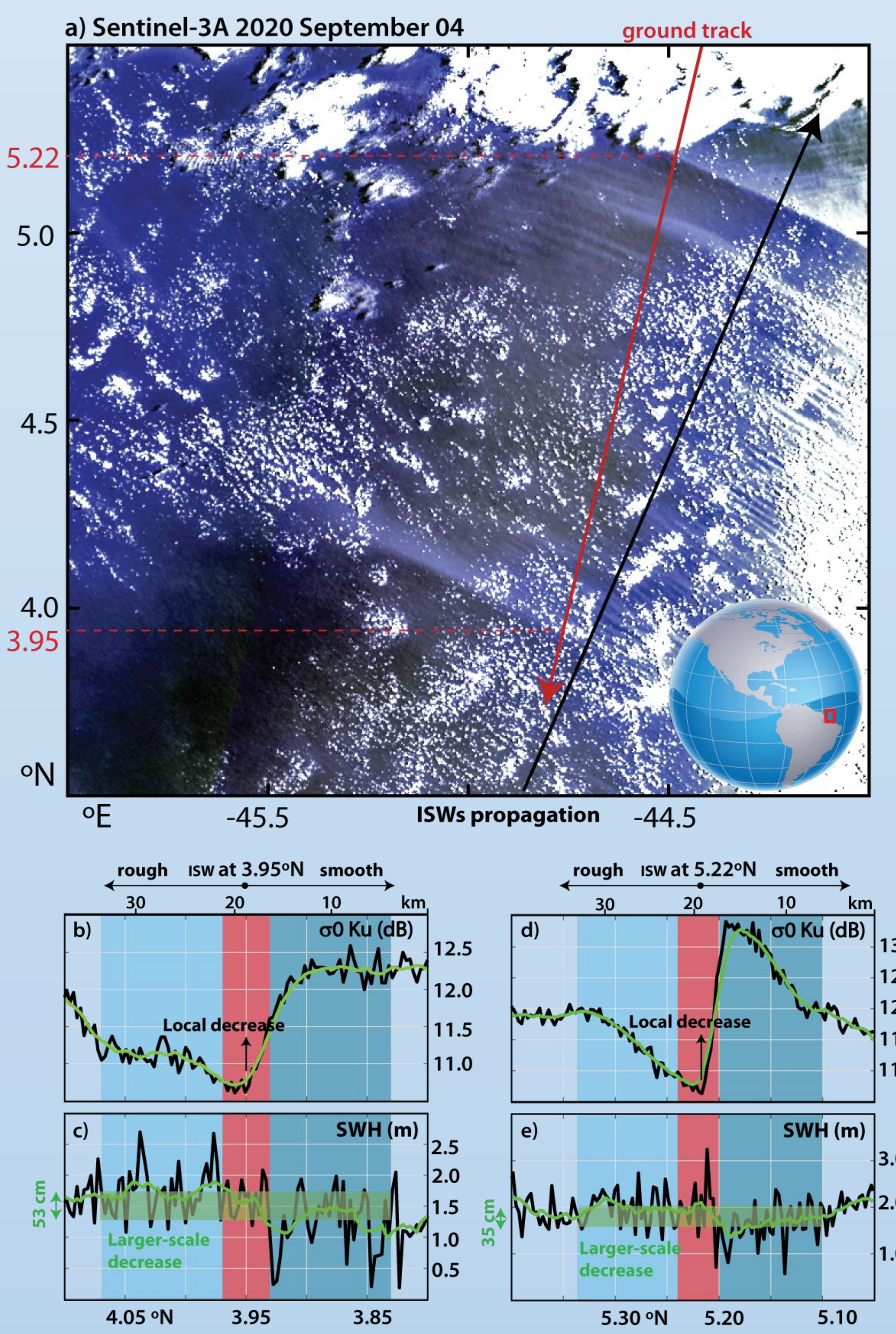

Fig. 1. (a) Quasi-true color (L1b) acquired by the OLCI (b) Along-track σ0 measured by the SRAL altimeter (in synergy with the OLCI) showing variations of approximately 2 dB in the leading ISW around 3.95°N. (c) SWH for the same ISW showing a larger-scale variation of 0.53 meters. (d) Along-track σ0 showing variations of approximately 3 dB in the leading ISW around 5.22°N. (e) SWH for the same ISW showing a larger-scale variation of 0.35 meters.

Results of New data UF SAR 20 Hz and FF SAR 160 Hz

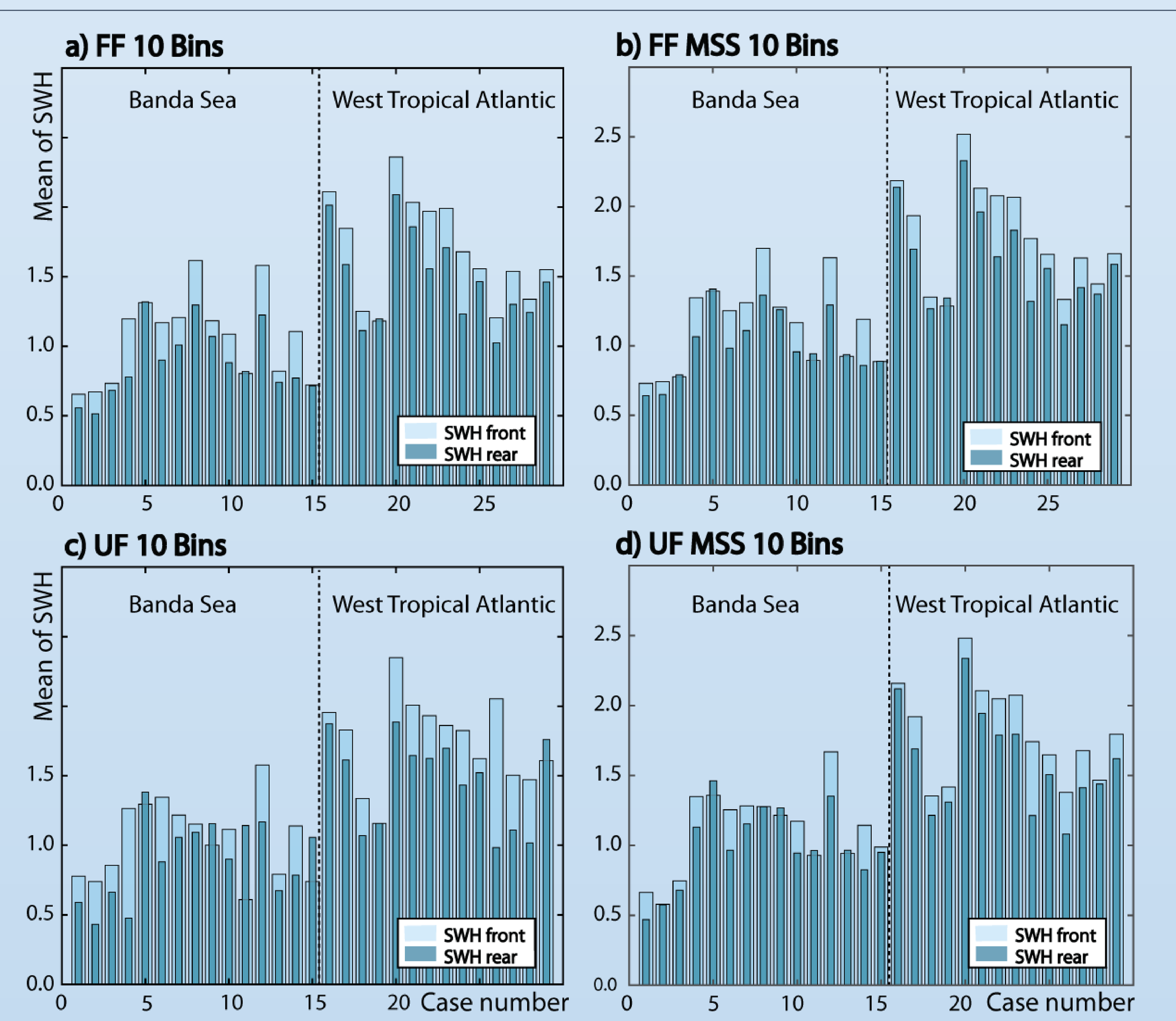

Fig. 2. Bar plots of SWHs leading (front) and trailing (rear) sections of the ISWs for our selected cases : (a) FF 10 Bins. (b) FF MSS 10 Bins. (c) UF 10 Bins. (d) UF MSS 10 Bins.

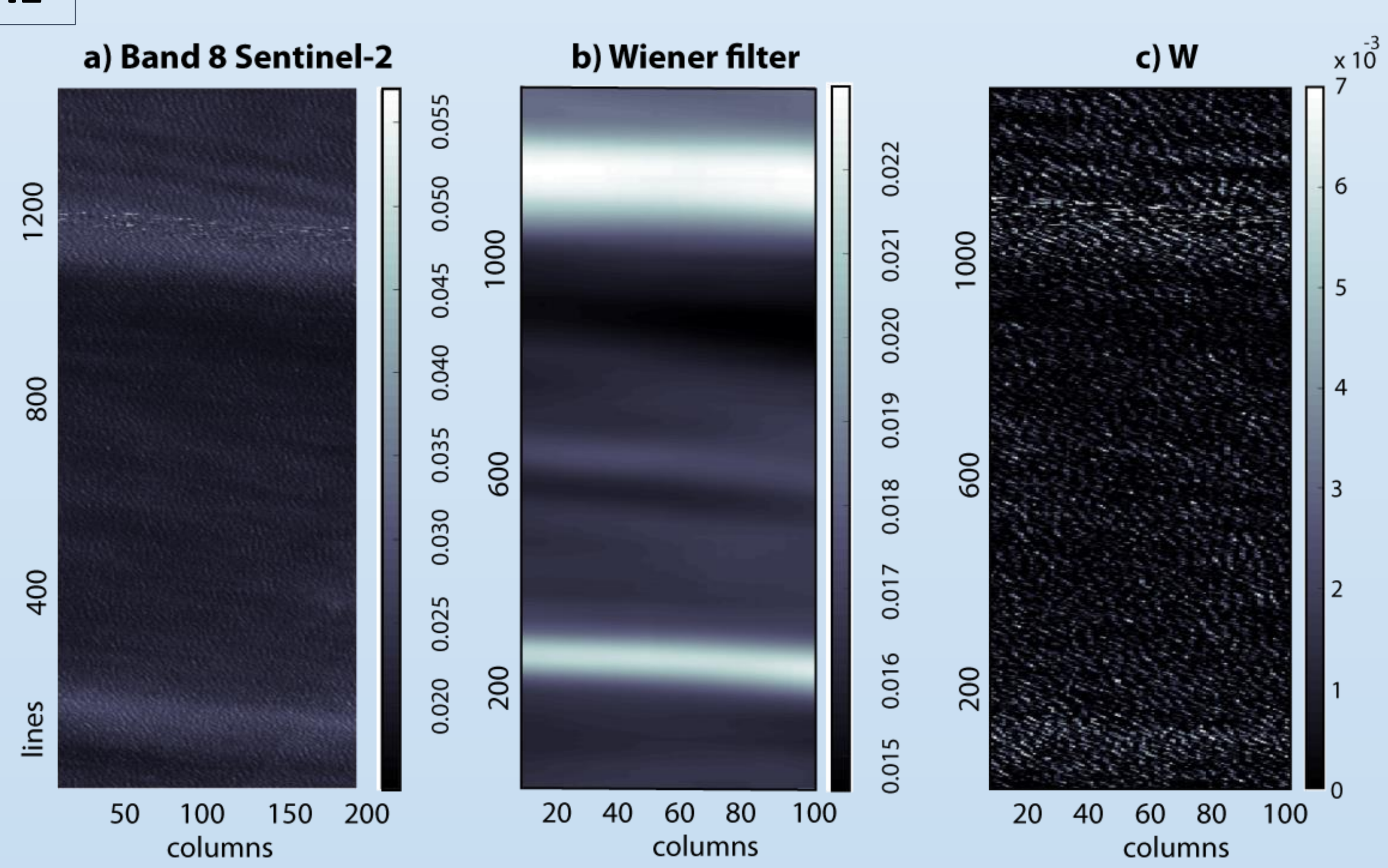

Fig. 4. (a) Zoom as shown in the black rectangle in Figure 3b corresponding to the NIR Band 8 of the Multispectral Instrument (MSI) showing sea surface signatures of an ISW packet. (b) Wiener filter applied to the image in part (a) – see Kubryakov et al., 2021 for details. (c) The image labelled W represents the wave breaking fraction, calculated by subtracting part (b) from (a).

Image processsing for the investigation of wave breaking in Sentinel-2 images

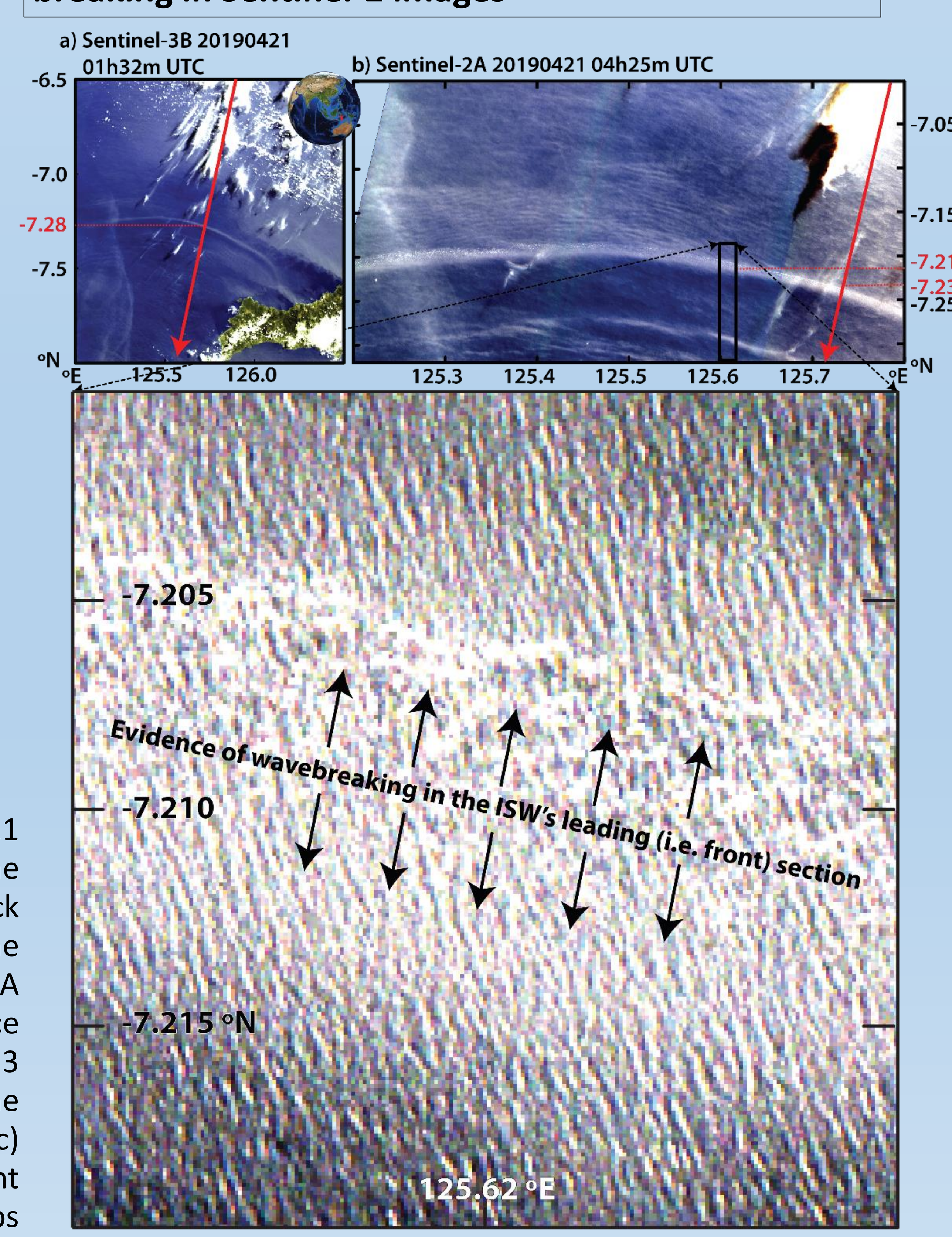

Fig. 3. (a) Quasi-true color image (Level-1b) acquired on 21 April 2019 at 01h31m UTC by the OLCI sensor onboard the Sentinel-3B satellite. The red line represents the ground-track of the satellite. (b) Image taken in the visible band by the Multispectral Instrument (MSI) on-board the Sentinel-2A satellite on 21 April 2019 at 04:25 UTC showing sea surface signatures of the same ISW packet seen in (a) approximately 3 hours later. The red line also represents the ground-track of the satellite Sentinel-3 in the same day but at a different time. (c) Zoomed section of the leading ISW seen in (b). Note the bright spots aligned in bands, which are evidence of whitecaps generated by breaking surface waves.

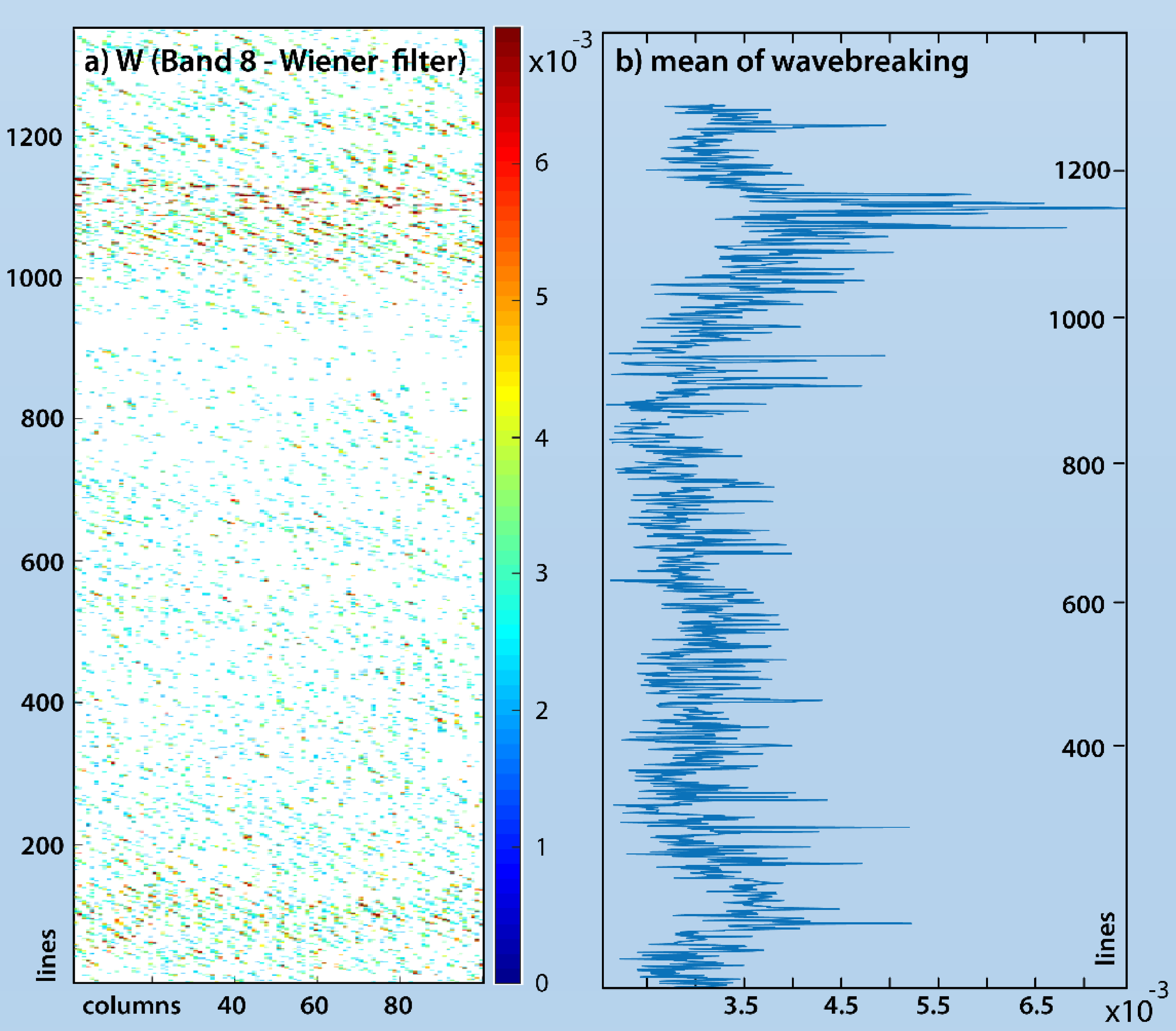

Fig. 5. (a) W represents wave breaking as shown in Figure 4c but color-coded to highlight the ISWs different sections, in which we applied a threshold of 0.002. (b) Mean of wave breaking fraction, i.e. W calculated for each line of (a), which is also approximately along the ISW's crests.

Acknowledgments: This work was funded by the EU and ESA, under subcontract CLS-ENV-BC-20-0017 "Multi Sensor Synergy Study for Sentinel-3C/D" between the University of Porto and Collecte Localisation Satellites, SA. J.C.B.dS. thanks the Portuguese funding agency Fundação para a Ciência e Tecnologia (FCT) under project UIDB/04683/2020. A.M.S-F. gratefully acknowledge FCT and the UE for a PhD grant SFRH/BD/143443/2019. J.M.M. thanks the FCT under projects UIDB/04423/2020 and UIDP/04423/2020.